EBioMedicine 44 (2019) 237–249

Contents lists available at ScienceDirect

EBioMedicine

journal homepage: www.ebiomedicine.com

EBioMedicine
Published by THE LANCET

NCAPG2 overexpression promotes hepatocellular carcinoma proliferation and metastasis through activating the STAT3 and NF-κB/miR-188-3p pathways

Fanzheng Meng [a,1], Shugeng Zhang [a,1], Ruipeng Song [b,1], Yao Liu [a,1], Jiabei Wang [b], Yingjian Liang [a], Jizhou Wang [b], Jihua Han [d], Xuan Song [a], Zhaoyang Lu [a], Guangchao Yang [a], Shangha Pan [c], Xianying Li [a], Yufeng Liu [a], Fang Zhou [a], Yan Wang [a], Yifeng Cui [a], Bo Zhang [a], Kun Ma [a], Congyi Zhang [a], Yufei Sun [a], Mengyang Xin [a], Lianxin Liu [a,*]

[a] Department of General Surgery, Key Laboratory of Hepatosplenic Surgery, Ministry of Education, The First Affiliated Hospital of Harbin Medical University, Harbin, China
[b] Department of General Surgery, Division of Life sciences and Medicine, The first Affiliated Hospital of University of Science and Technology, China
[c] Key Laboratory of Hepatosplenic Surgery, Ministry of Education, The First Affiliated Hospital of Harbin Medical University, Harbin, China
[d] Department of Head and Neck Surgery, The Third Affiliated Hospital of Harbin Medical University, Harbin, Heilongjiang, China

ARTICLE INFO

Article history:
Received 16 April 2019
Received in revised form 21 May 2019
Accepted 26 May 2019
Available online 5 June 2019

Keywords:
NCAPG2
Hepatocellular carcinoma
STAT3
NF-κB
miR-188-3p

ABSTRACT

Background: Hepatocellular carcinoma (HCC) is a highly fatal malignant cancer worldwide. Elucidating the underlying molecular mechanism of HCC progression is critical for the identification of new therapeutic targets for HCC. This study aimed to determine the role of Non-SMC condensin II complex subunit G2 (NCAPG2) in HCC proliferation and metastasis.

Methods: We detected NCAPG2 expression in tissues using immunohistochemistry, western blotting and real-time PCR. The effects of NCAPG2 on cell proliferation and metastasis were evaluated both *in vitro* and *in vivo*. Immunocytochemistry, enzyme linked immunosorbent assay, co-immunoprecipitation and luciferase reporter assay were performed to uncover the underlying mechanisms.

Findings: We found that NCAPG2 is frequently upregulated in HCC tumour tissues and predicts a poor prognosis. NCAPG2 overexpression promotes HCC proliferation, migration, and invasion through activating STAT3 and NF-κB signalling pathways. Moreover, *NCAPG2* is a direct target of miR-188-3p. We demonstrated the existence of a positive feedback loop between NCAPG2 and p-STAT3 and a negative feedback loop between NCAPG2 and miR-188-3p.

Interpretation: Our study indicates that NCAPG2 overexpression could drive HCC proliferation and metastasis through activation of the STAT3 and NF-κB/miR-188-3p pathways. These findings may contribute to the identification of novel biomarkers and therapeutic targets for HCC.

Fund: National Key Program for Science and Technology Research and Development (Grant No. 2016YFC0905902); the National Natural Scientific Foundation of China (Nos. 81772588, 81602058, 81773194); University Nursing Program for Young Scholars with Creative Talents in Heilongjiang Province (Grant No. UNPYSCT-2016200); the Innovative Research Program for Graduate of Harbin Medical University (Grant Nos. YJSCX2017-38HYD, YJSCX2016-18HYD).

1. Introduction

Hepatocellular carcinoma (HCC) is a highly fatal malignant cancer that is the fourth leading cause of cancer-related mortality worldwide [1]. Most patients only receive a confirmed diagnosis of HCC at an advanced stage and, therefore, miss the optimal time for radical treatment, especially in less developed countries. Even with excellent treatment, the overall prognosis for HCC is poor due to early recurrence or metastasis [2,3]. Therefore, it is important to investigate and understand the

* Corresponding author at: Department of General Surgery, Key Laboratory of Hepatosplenic Surgery, Ministry of Education, the First Affiliated Hospital of Harbin Medical University, #23 Youzheng Street, Harbin 150001, Heilongjiang Province, China.
E-mail address: liulianxin@ems.hrbmu.edu.cn (L. Liu).
[1] These authors contributed equally to this work.

https://doi.org/10.1016/j.ebiom.2019.05.053

Research in context

Evidence before this study

NCAPG2 belongs to chromosome condension II complex, which is critical for mitosis, DNA repair and histone modulation. Our mRNA microarray analysis (using 5 paired tumours and adjacent tissues from HCC patients) indicated that NCAPG2 is obviously upregulated in HCC tumours. However, whether NCAPG2 has a functional effect and how NCAPG2 is regulated during HCC progression are yet to be elucidated.

Added value of this study

NCAPG2 is an important oncogene that contributes to HCC proliferation and metastasis through upregulating NF-κB pathway, IL-6 secretion, activating STAT3 and its target genes (including c-myc, CDK4, cyclin D1, Slug, MMP 9). Furthermore, there existes a positive feedback loop between NCAPG2 and p-STAT3 and a negative feedback loop between NCAPG2 and miR-188-3p.

Implications of all the available evidence

This study has great potential for expanding our knowledge of NCAPG2 and miR-188-3p during HCC progression and provides novel biomarkers and therapeutic targets for HCC patients.

underlying molecular mechanism of HCC progression to identify new therapeutic targets.

Non-SMC condensin II complex subunit G2 (NCAPG2) belongs to the chromosome condensin II complex, which is critical for chromosome condensation and segregation during mitosis. Phosphorylation-dependent PHF8 dissociation from chromatin in prophase leads to the interactions between the HEAT repeat clusters in NCAPG2 and H4K20me1 during cell cycle progression [4]. Previous studies indicate that NCAPG2 interacts with Polo-like kinase 1 (PLK1) during the prometaphase-metaphase transition in mitosis, and is a critical player in PLK1 kinetochore localization [5]. PLK1 is a well-established oncogene in HCC progression [6]. Recently, it was demonstrated that NCAPG2 promotes tumour proliferation by regulating the G2/M phase and is associated with poor prognosis in lung adenocarcinoma [7]. However, whether NCAPG2 plays a role during HCC progression is yet to be determined.

MicroRNAs participate in many biological processes including HCC progression by directly interacting with mRNAs and inhibiting expression of the target genes *via* various molecular mechanisms [8,9]. Aberrant miRNAs can act as oncogenes or tumour suppressor genes by downregulating specific target genes, including pivotal signalling pathway factors, which may be involved in epigenetic modifications [10], cancer stem cells (CSCs) [11], epithelial-to-mesenchymal transition (EMT) [12], matrix metalloproteinases (MMPs) activity [13], and other signalling pathways.

Chronic inflammation is one of the main risk factors for cancer. In addition to producing secreted inflammatory cytokines, including interleukin-1β (IL-1β) and interleukin-6 (IL-6), chronic inflammation generates cascade activation of corresponding transcription factors involved in carcinogenesis or metastasis, such as NF-κB and STAT3 [14,15]. Our previous study suggested that NF-κB acts as a direct transcriptional regulator of ATPase Inhibitory Factor 1 (ATPIF1) expression, and ATPIF1 in turn upregulates NF-κB activation and Snail and VEGF expression to promote metastasis and angiogenesis in HCC [16]. In human HCC, expression of p-STAT3 is upregulated, and p-STAT3 cooperates with NANOG to activate Twist 1 resulting in TLR4-mediated liver tumorigenesis [17]. In addition, NF-κB and STAT3 can mutually regulate each other [18,19]. NF-κB generates high levels of IL-6 by directly activating IL-6 transcription, and high levels of IL-6 in turn activates NF-κB, thereby completing the positive feedback loop that maintains the transformed phenotype, self-renewal of mammospheres, and tumour formation [20].

In this study, we demonstrated that increased NCAPG2 and reduced miR-188-3p expression levels are associated with HCC progression and poor prognosis. NCAPG2 overexpression stimulates the phosphorylation of STAT3, which directly enhances NCAPG2 transcription. Moreover, NCAPG2 is a target of miR-188-3p, which can be negative regulated by NF-κB activation resulting from increased NCAPG2, thus forming a negative feedback loop. Altogether, our study provides a novel signalling pathway that mediates HCC progression produced by NCAPG2 and miR-188-3p.

2. Materials and methods

2.1. Clinical specimens and cell lines

Two independent cohorts composed of 216 patients with HCC were enrolled in this study (cohort 1, $n = 136$; cohort 2, $n = 80$). Paired HCC tissues and adjacent liver tissues were collected from patients who underwent liver resection at the First Affiliated Hospital of Harbin Medical University between January 2008 and August 2013. All patients provided written informed consent and this study was approved by the Research Ethics Committee of the First Affiliated Hospital of Harbin Medical University. Follow-up data were collected from patients after hepatic resection to monitor and assess the overall rate of cancer metastasis and recurrence. A normal liver cell line (L02) and several HCC cell lines (Huh7, HCCLM3, SK-Hep-1, MHCC97H, MHCC97L, SMMC7721, and HepG2) were purchased from Shanghai Cell Bank of Chinese Academy of Sciences (Shanghai, China).

2.2. Lentivirus and shRNA transfection

The lentiviral vector system (LV), short hairpin RNAs (LV-shRNA) and the empty vectors were purchased from GeneChem Corporation (Shanghai, China). Oligonucleotides for mimics, inhibitors and negative-control were purchased from RiboBio Corporation (Guangzhou, China). The specific sequences were displayed in Supplementary Table 2. Transfection of plasmids (2 μg mimics, 150-200 nM inhibitors or siRNAs) were transfected into according to the manufacturer's suggested protocols.

2.3. Immunohistochemical (IHC) analysis

Sample and microarray sections were stained with diaminobenzidine (DAB Kit; Vector Laboratories) and counterstained with hematoxylin (Sigma, St. Louis, MO, USA) to visualize the immunoreaction product following the manufacturer's suggested protocols. Briefly, the percentage score was defined as: 0, 0 to <5%; 1, 5 to <25%; 2, 26 to <50%; 3, 51 to 75%; 4, 76 to 100%; the staining intensity was defined as 1, weak; 2, moderate; 3, strong and providing a Multiply index (MI) score (MI = intensity* percentage) as follows: MI, 0, scored as 1; MI, 1–4, scored as 2; MI, 5–8, scored as 3; MI, 9 or 12, scored as 4. Samples with a score equal to or ≥ 3 were considered to exhibit high expression, while those with a score ≤ 2 were classified as showing relative low expression.

2.4. Quantitative real-time PCR and western blot analysis

Quantitative real-time PCR and western blot analyses were performed as previously described [21]. Detailed information regarding the primers used for quantitative real-time PCR is listed in

Supplementary Table 4. Information on all the primary antibodies used in this study is provided in Supplementary Table 3.

2.5. Proliferation and Transwell assays

Cell growth, colony formation, migration, and invasion assays were performed according to the manufacturer's instructions as described in previous studies [21]. As for the cell cycle tests, 20×10^4 transfected cells were fixed in 80% ethanol overnight and stained as the protocol of Cycle TESTTM PLUS DNA Reagent Kit (BD Biosciences San Jose, CA) and were analysed by flow cytometry (Beckman Coulter FC500).

2.6. Wound-healing assay

Transfected Cells were seeded in a 6-well plate at 30×10^4cells per well. After the cells attached completely, a 10-μl pipette tip was used to scratch a straight line in each well and then washed with PBS and cultured in serum-free medium for additional 24 or 36 h, the scratch lines were captured by using microscopic camera.

2.7. Immunofluorescence (IF) assay

Cells were seeded on polylysine-coated coverslips, cultured for 24 h, and fixed with 4% paraformaldehyde, followed by 0.1% Triton-X-100 permeabilization. Then cells were incubated with primary antibodies, secondary antibodies (Invitrogen) and DAPI (Vector Laboratories) in sequence. The images were captured under microscopic camera.

2.8. In Vivo tumour growth and metastasis assays

All experimental protocols involving animals were approved by the Animal Ethics Committee of Harbin Medical University, China. Four- to six-week old male BALB/c nude mice were purchased from the Shanghai Animal Centre (Shanghai, China). Flank subcutaneous xenografts were established by subcutaneous injection of 1×10^6 cells suspended in 100 μl PBS. After 4 weeks, subcutaneous tumours were removed and their volume and weight recorded. For the liver orthotopic xenograft implantation model, subcutaneous tumours were dissected into 1-mm^3 sections and then implanted into the liver parenchyma. Tumour growth was monitored by bioluminescent signals, and mice were sacrificed after 6 weeks. Moreover, 1×10^6 cells were injected into the mouse tail vein to achieve *in vivo* lung metastasis. The metastatic nodules were also measured by bioluminescent signals and the mice were sacrificed after 6 weeks. Tumour, liver, and lung sections were processed for hematoxylin and eosin (H&E) staining and immunohistochemistry (IHC) to assess proliferation and metastasis potential.

2.9. Luciferase reporter assay

Luciferase reporter assays were performed according to the manufacturer's instructions (Promega). To determine the influence of p-STAT3 on *NCAPG2* promoter activity, the *NCAPG2* promoter-luciferase reporter plasmids containing NCAPG2 promoter region from 3014–3100 bp upstream of its transcription start site were constructed in the pGL3.0 plasmid. To evaluate the interaction between miR-188-3p and NCAPG2, the indicated cells were transfected with pGL3-based constructs containing *NCAPG2*-WT or *NCAPG2*-MUT plus miR-188-3p mimics or inhibitors. Twenty-four hours after transfection, firefly and Renilla luciferase activity was examined by the Dual-Luciferase Reporter Assay System (Promega). Renilla activity was used to normalise firefly activity.

2.10. Co-immunoprecipitation (IP) assay

Cells were harvested and then lysed in 500 μl co-IP buffer containing a protease inhibitor cocktail (Sigma-Aldrich). After centrifugation, cell lysates were collected and precleared by incubating with 20 μl immobilized protein A/G beads for 1 h at 4 °C. The beads were then discarded using a magnetic frame and the lysates incubated with primary antibody or control IgG on a rotator at 4 °C overnight. On the following day, 20 μl of immobilized protein A/G beads were added to precipitate the protein complex at 4 °C for 4 h. Subsequently, samples were washed five times, the beads were boiled in loading buffer, and the proteins were prepared for western blotting as described above.

2.11. Chip-qPCR

The process was followed by formaldehyde fixation (1% final concentration), cell lysis, and sonication and the immunoprecipitation were performed using STAT3 antibody. The PCR products were separated by agarose gel electrophoresis and visualized by ethidium bromide staining. Detailed information regarding the primers used for Chip-PCR is listed in Supplementary Table 4.

2.12. ELISA assay

IL-6 concentrations were measured *via* ELISA Kit (Boster Biological Technology, Wuhan, China. Catalog #EK0410). ELISA experiments were performed according to manufacturer's instructions. Supernatant was centrifuged before use and stored at −80 °C. Cytokine concentrations were normalized to cell counts in each well.

2.13. Statistical analyses

Each experiment was performed three times. Clinical information of The Cancer Genome Atlas (TCGA) for liver cancer was downloaded from the TCGA database (https://tcga-data.nci.nih.gov/; accessed on February 6, 2016). Statistical analyses was performed with SPSS 19.0 software or GraphPad Prism 7.0 software. Data are presented as mean ± standard deviation (SD), and the Student's *t*-test or one-way or two-way ANOVA was used to compare the means of independent samples. Correlations were determined using Pearson's linear-regression analysis. The log-rank test was used to compare Kaplan–Meier survival curves. *P* values of <0.05 were considered statistically significant.

3. Results

3.1. NCAPG2 is frequently upregulated in HCC and predicts a poor prognosis

Our mRNA microarray analysis (using 5 paired tumour and adjacent tissues from patients with HCC) indicated that NCAPG2 is significantly upregulated in HCC tumours ($P = .0017$, FC = 2.933449, Supplementary Fig. 1a). To further confirm the clinical significance of NCAPG2 expression in patients with HCC, we examined a tissue microarray cohort of 136 patients with HCC using IHC staining and western blotting with an NCAPG2 antibody (Fig. 1a, b). The expression level of NCAPG2 was significantly higher in HCC tumour tissues than adjacent non-tumour tissues, and the NCAPG2 staining was more intense in more advanced-stage liver cancer (Supplementary Fig. 1b). Moreover, a clinicopathological characteristic analysis indicated that higher NCAPG2 expression is positively associated with tumour size ($P = .0022$), TNM stage ($P = .0193$), vascular invasion ($P = .0036$), and lymph node metastasis ($P = .0304$) (Fig. 1c and Supplementary Table 1). The expression levels of *NCAPG2* mRNA were also validated in the other cohort of patients with HCC (80 paired specimens) using real-time PCR (Fig. 1d). Intriguingly, worse overall survival (OS) and disease-free survival (DFS) were usually accompanied by higher NCAPG2 expression in patients with HCC (Fig. 1e, f), which is consistent with the TCGA dataset analysis (Supplementary Fig. 1c-e). These results indicated that NCAPG2 is frequently upregulated in patients with HCC and may act as a predictor for HCC survival and recurrence.

3.2. NCAPG2 enhances HCC cell proliferation in vitro and in vivo

Prior to the functional tests, we examined *NCAPG2* mRNA and protein expression levels in HCC cell lines with different metastatic potency. Compared to a normal liver cell line (L02), much higher expression was detected in the HCC cell lines, especially in the highly metastatic HCCLM3 and SK-Hep1 cells (Fig. 2a, b). Next we designed gain- and loss-of-function studies by overexpressing NCAPG2 in Huh7 cells and knocking down NCAPG2 expression in HCCLM3 and SK-Hep1 cells by lentivirus (Lv) transfection. We verified and chose Lv-shRNA 78–1 and 80–1 as the best candidates for silencing NCAPG2 expression by western blotting (Fig. 2c). In CCK8 growth curve assays, NCAPG2 overexpression significantly increases cell growth, whereas silencing NCAPG2 decreases cell growth from the fourth day after lentivirus transfection (Fig. 2d). Colony formation assays showed that NCAPG2 overexpression contributes to increased colony size and numbers, while knocking down NCAPG2 impairs the foci formation capacity (Fig. 2e and Supplementary Fig. 3a). Subsequently, a cell cycle analysis reveals that NCAPG2 upregulation in Huh7 cells enhances the G1/S transition, while NCAPG2 downregulation in HCCLM3 and SK-Hep1 cells inhibits the transition (Fig. 2f). No ideal results were achieved by analysis of apoptosis assays (Supplementary Fig. 2). The *in vivo* experiments were conducted in a subcutaneous and liver tumour orthotopic nude mouse model. The results revealed a similar trend to what was observed *in vitro*; Huh7-NCAPG2 cells are more likely to generate higher tumour volumes and growth rates, whereas HCCLM3-sh NCAPG2 cells decrease the tumorigenicity to a certain extent (Fig. 2g). In addition, we found that overexpression of NCAPG2 in Huh7-derived orthotopic tumours gave rise to more intrahepatic metastatic nodules than the control group. Silencing NCAPG2 in the HCCLM3 model resulted in fewer liver metastatic nodules. Furthermore, compared with the control group, overexpression of NCAPG2 resulted in stronger Ki67 staining in liver orthotopic tumour sections, while silencing NCAPG2 expression produced the opposite results (Fig. 2h, i). Taken together, our findings indicate that NCAPG2 plays an important role in facilitating HCC proliferation *in vitro* and tumorigenesis *in vivo*.

3.3. NCAPG2 promotes HCC cell migration, invasion, and lung metastasis

Given the positive association between NCAPG2 and TNM stage, vascular invasion, and lymph node metastasis, we decided to investigate whether NCAPG2 expression affects HCC cell motility and invasiveness. Wound-healing tests showed that when NCAPG2 is upregulated in Huh7 cells, cell migratory ability is enhanced, but the ability is abrogated when NCAPG2 is silenced in HCCLM3 and SK-Hep1 cells (Fig. 3a and Supplementary Fig. 3b). Overexpression of NCAPG2 increases the migratory and invasive capabilities of Huh7 cells significantly, as revealed by Transwell migration and Matrigel invasion assays. In contrast, knocking down NCAPG2 in the highly invasive HCCLM3 and SK-Hep1 cells decreases their motility and invasive behaviours (Fig. 3b, c and Supplementary Fig. 3c).

To determine whether NCAPG2 could affect HCC metastasis *in vivo*, we injected stable transfected cells (Huh7-NCAPG2, HCCLM3-shNCAPG2, and controls) through the tail vein of nude mice and monitored for lung metastatic nodules. Six weeks after injection, the mice in the Huh7-NCAPG2 group exhibited more and bigger lung metastatic nodules than the HCCLM3-shNCAPG2 group (Fig. 3d-f). The presence of the lung metastatic nodules was confirmed by H&E staining (Fig. 3g). IHC staining of epithelial-mesenchymal transition (EMT) markers showed that the Huh7-NCAPG2 derived lung metastatic nodules have a relatively lower expression of E-cadherin and higher expression of N-cadherin and vimentin compared to the nodules from the Huh7-con group. While HCCLM3-shNCAPG2 group displayed an opposite compared to control group (Supplementary Fig. 4). These results provide further evidence that NCAPG2 is involved in promoting HCC invasion and metastasis.

3.4. NCAPG2 induces epithelial–mesenchymal transition in HCC

EMT is a cellular process characterised by a loss of epithelial characteristics and gain of mesenchymal phenotypes, which drives epithelial cells to acquire motility and invasiveness. Thus, we sought to investigate the relationship between NCAPG2 and EMT in HCC. Western blotting data showed that NCAPG2 overexpression in Huh7 cells decreases the expression of the epithelial marker E-cadherin, and upregulates the expression of the mesenchymal markers, N-cadherin and vimentin. The opposite result was obtained in HCCLM3-shNCAPG2 and SK-Hep1-sh NCAPG2 cells when compared to controls, as evidenced by PCR and immunofluorescence (IF) analyses (Fig. 4a, b). Moreover, the IF staining of phalloidine revealed that Lv-NCAPG2-transfected Huh7 cells tend to exhibit a more spindle-like, mesenchymal morphology. In contrast, Lv-shRNA-NCAPG2-transfected HCCLM3 and SK-Hep1 cells appear round, with a more epithelial morphology than Lv-shRNA-control cells (Fig. 4c). Previous studies have demonstrated that EMT markers can be regulated by transcription factors such as Snail, Slug, Twist, and Zeb1 family proteins [22,23]. Our results revealed that only Slug protein and mRNA levels were significantly increased after NCAPG2 overexpression, while the opposite was observed after NCAPG2 expression knockdown (Fig. 4a and Supplementary Fig. 5a, b). The same trend was further confirmed by IF (Fig. 4c). Taken together, these observations suggest that NCAPG2 induces EMT in HCC cells.

3.5. Slug is essential for NCAPG2-mediated EMT and HCC metastasis

We next examined the role of Slug in NCAPG2-mediated EMT progression. We found that knocking down slug expression using shRNA-slug in Huh7 cells markedly attenuates the decrease in E-cadherin and inhibits the increase of N-cadherin and vimentin induced by NCAPG2 overexpression. In contrast, overexpression of Slug inhibits E-cadherin upregulation and rescues the loss of N-cadherin and vimentin expression in HCCLM3-shNCAPG2 cells (Fig. 4d). Functional tests of Slug were then conducted *in vitro* and *in vivo* using stable lentivirus transfection. As expected, we found that the migration and invasiveness of Huh7-NCAPG2 cells was repressed by knocking down Slug expression, while the decreased migratory and invasive capabilities of HCCLM3-shNCAPG2 cells were restored by ectopic overexpression of Slug (Fig. 4e). In addition, we found fewer and smaller lung metastatic nodules in mice injected with Huh7-NCAPG2-sh Slug cells compared to Huh7-NCAPG2-sh control cells. In contrast, the Lv-shRNA-NCAPG2-mediated decrease in lung metastatic nodules was significantly reversed by Slug overexpression in the HCCLM3 group (Fig. 4f, g). These observations were further confirmed by H&E staining of the lung sections (Fig. 4h). Our results indicated that Slug likely plays a critical role in NCAPG2-induced EMT and metastasis in HCC cells.

3.6. NCAPG2 exerts dual functions by activating the STAT3 and NF-κB signalling pathways

Given the obvious effects of NCAPG2 on HCC cell growth and metastasis, we examined the relationship between NCAPG2 and signalling pathways that regulate tumour growth and metastasis, including the NF-κB, STAT3, protein kinase B (AKT), and extracellular signal-regulated kinase (ERK) pathways. Western blot analyses showed that total protein levels of NF-κB, p-NF-κB (S536), p-STAT3 (Y705), and other targets (c-myc, CDK4, cyclin D1, MMP9) are increased by NCAPG2 overexpression and decreased by NCAPG2 silencing (Fig. 5a; Supplementary Fig. 5c). However, the quantification of p-NF-κB/NF-κB did not reach statistical significance (Supplementary Fig. 5d). The mRNA levels of NF-κB, c-myc, cyclin D1, CDK4, and MMP9 are upregulated by NCAPG2 overexpression, and downregulated by silencing NCAPG2 expression in HCC cells (Supplementary Fig. 5e). Examining the expression of these proteins in the liver orthotopic and lung metastasis tumour tissues produced results similar to the *in vitro* observations

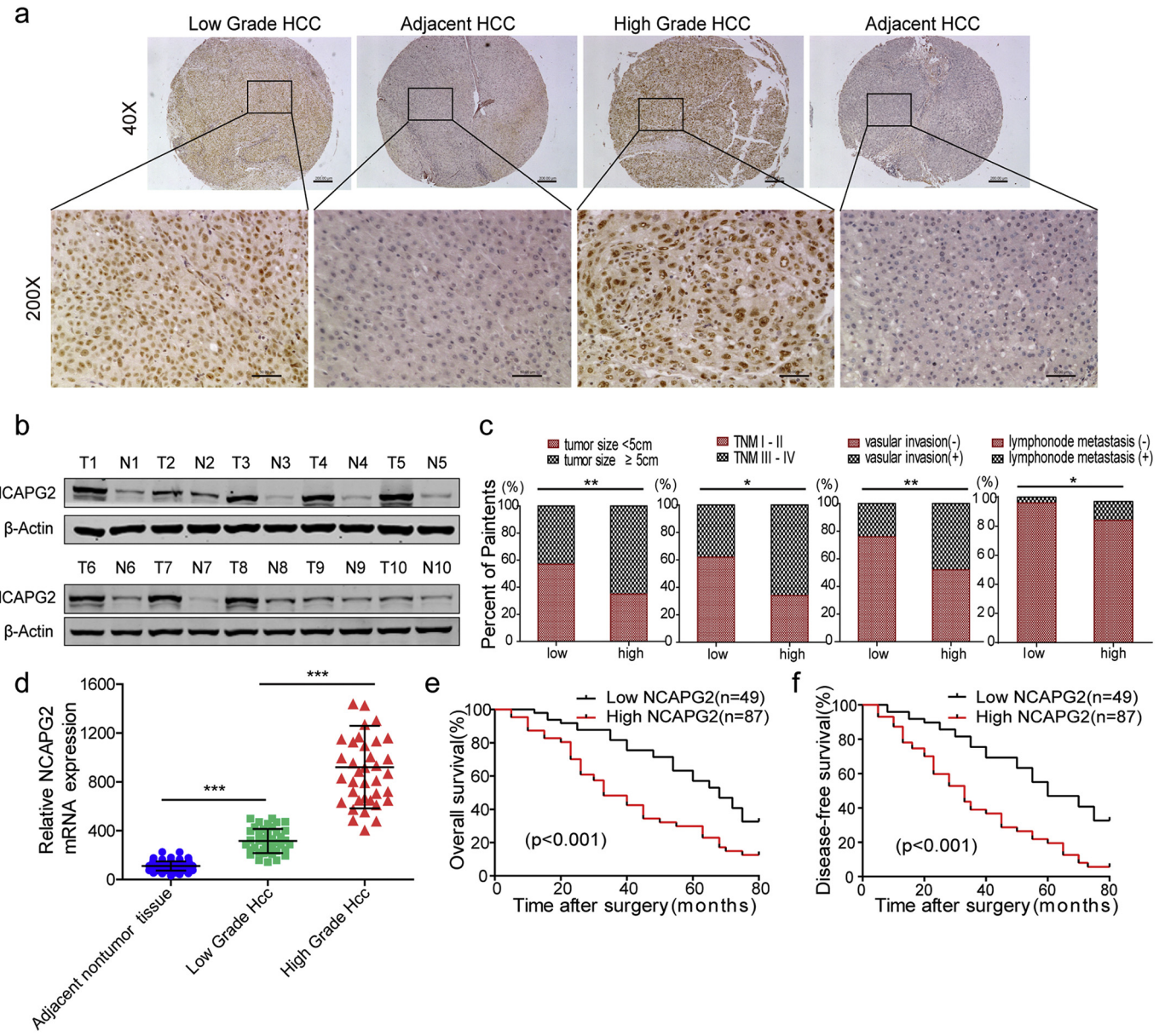

Fig. 1. NCAPG2 is frequently upregulated in HCC and is a promising prognostic biomarker for HCC. (a) Representative images of NCAPG2 IHC staining in HCC and normal liver tissues. (b) Representative images of western blotting of NCAPG2 in HCC and adjacent normal liver tissues. T: tumours; N: adjacent normal tissues. (c) Percentage of patients with relative high expression and low expression of NCAPG2 according to these clinical parameters: (1) tumour size, (2) tumour stage, (3) vascular invasion, (4) lymph node metastasis. (d) *NCAPG2* mRNA levels were analysed in 80 paired HCC and adjacent normal liver tissues by real-time PCR. (e-f) Kaplan-Meier plot of OS and DFS of patients with HCC with relatively high or low NCAPG2. All experiments were performed three times and data are presented as mean ± SD. $^{*}p < .05$; $^{**}p < .01$; $^{***}p < .001$.

(Supplementary Fig. 6a, b). The NF-κB and STAT3 signalling pathways have been confirmed to be closely related to HCC growth and metastasis [17,24–26], with IL-6 as a key factor influencing the crosstalk between NF-κB and IL-6/STAT3 signalling [20,27]. Detecting IL-6 secretion by ELISA showed that NCAPG2 overexpression tends to stimulate IL-6 secretion while knocking down NCAPG2 expression exerts the opposite effect (Fig. 5b). Next, we examined whether NCAPG2-mediated HCC growth and metastasis is dependent on the activation of STAT3. Preincubation of Huh7-NCAPG2 cells with the STAT3 inhibitor Stattic (10 μM, 24 h) resulted in the downregulation of c-myc, CDK4, cyclin D1, and Slug expression. However, in HCCLM3 cells, IL-6 stimulation (10 ng/ml, 24 h) increases the expression of p-STAT3 and rescues the shRNA-NCAPG2-mediated loss of c-myc, cyclin D1, CDK4, and Slug expression (Fig. 5c). We conclude that the STAT3 and NF-κB signalling pathways are crucial for NCAPG2-mediated HCC growth and metastasis.

3.7. P-STAT3 contributes to the upregulation of NCAPG2 expression in HCC cells

In our investigation of p-STAT3-mediated HCC progression, we found that NCAPG2 expression was also regulated by STAT3 activation and inactivation. To verify the relationship between p-STAT3 and NCAPG2, we performed a co-IP experiment, which confirms that p-STAT3 interacts with NCAPG2 (Fig. 5d and Supplementary Fig. 7a). Moreover, STAT3 chip-sequence data retrieval and bioinformatics analysis revealed that the promotor region of NCAPG2 contains conserved STAT3-binding sites [28]. In the present study, a Chip-qPCR assay showed that STAT3 is recruited to the region of the NCAPG2 promoter regulatory region when compared to the IgG group (Fig. 5e; Supplementary Fig. 7b, c). To determine the influence of p-STAT3 on NCAPG2 promoter activity, we performed a promoter

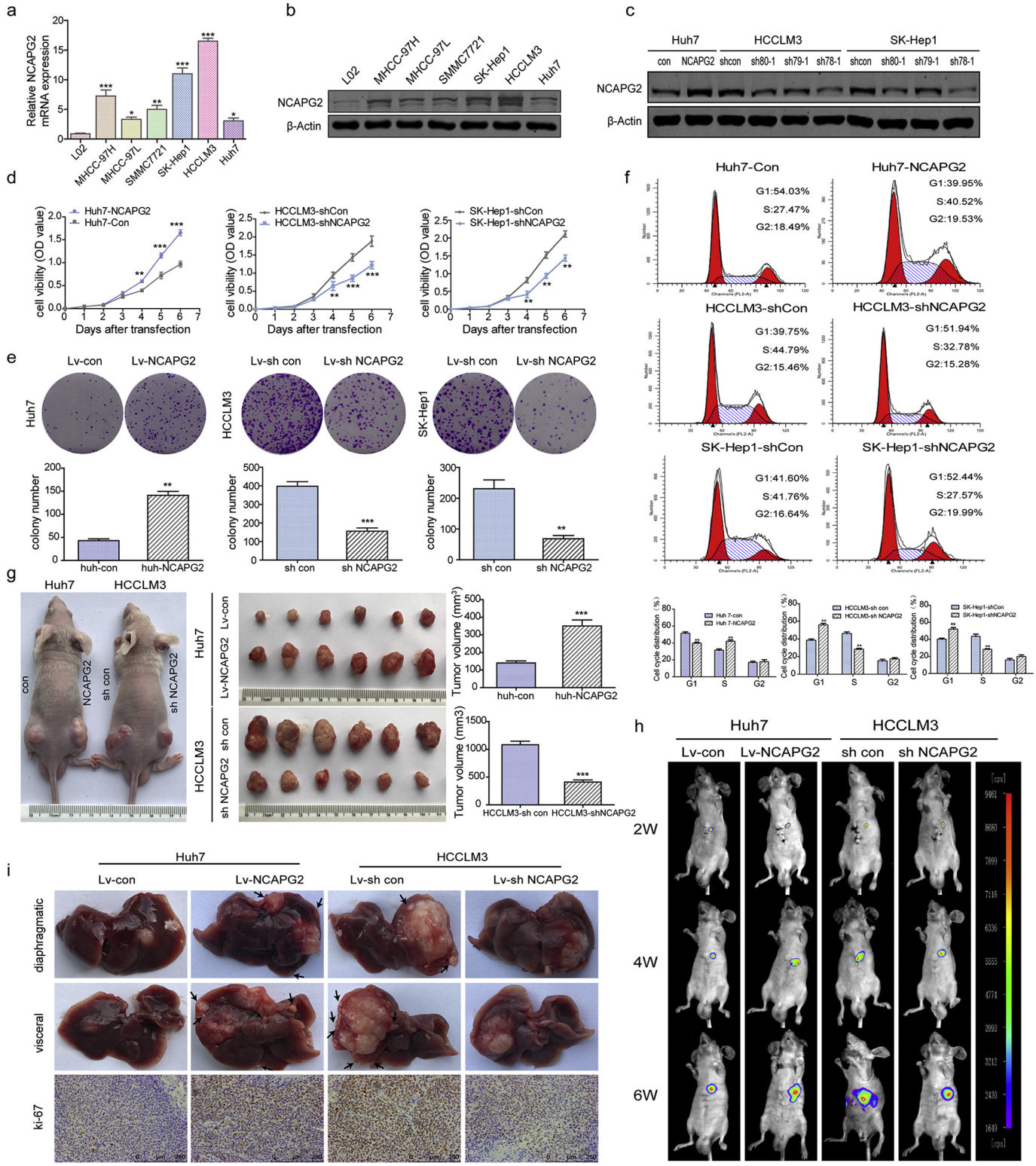

Fig. 2. NCAPG2 promotes proliferation and tumorigenesis *in vitro* and *in vivo*. (a) Real-time PCR analysis of *NCAPG2* mRNA levels in HCC cells compared to L02 cells. (b) Western blot analysis of NCAPG2 expression in L02 and HCC cells. (c) Western blot analysis of NCAPG2 expression after lentiviral transfection. (d) Growth curve assay based on CCK8 analysis in HCC cells. (e) Representative images of colony formation are shown in the upper panel and statistical analysis of colony numbers are in the lower panel. (f) Representative images of the cell cycle analysis of indicated HCC cells and statistical analysis in the lower panel; NCAPG2 knockdown blocked the G1/S transition. (g) Representative images of subcutaneous xenograft derived from indicated HCC cells. (h) Representative bioluminescence imaging of the liver tumour orthotopic model in a consecutive time (6 weeks). (i) Representative images of liver specimens and Ki67 IHC staining in liver tumour orthotopic models. NCAPG2 overexpression is accompanied by more intrahepatic metastasis, while NCAPG2 knockdown suppresses intrahepatic metastasis. All experiments were performed three times and data are presented as mean ± SD. $^{*}p < .05$; $^{**}p < .01$; $^{***}p < .001$.

luciferase assay with HCCLM3 cells transfected with NCAPG2-promoter-luc or pGL3-luc plasmids, respectively. The cells were treated with either IL-6 or Stattic. NCAPG2 promoter activity was significantly increased in IL-6-treated cells and obviously decreased by Stattic treatment, while no significant changes were observed in pGL3 Luciferase activity(Fig. 5f). Furthermore, NCAPG2 expression

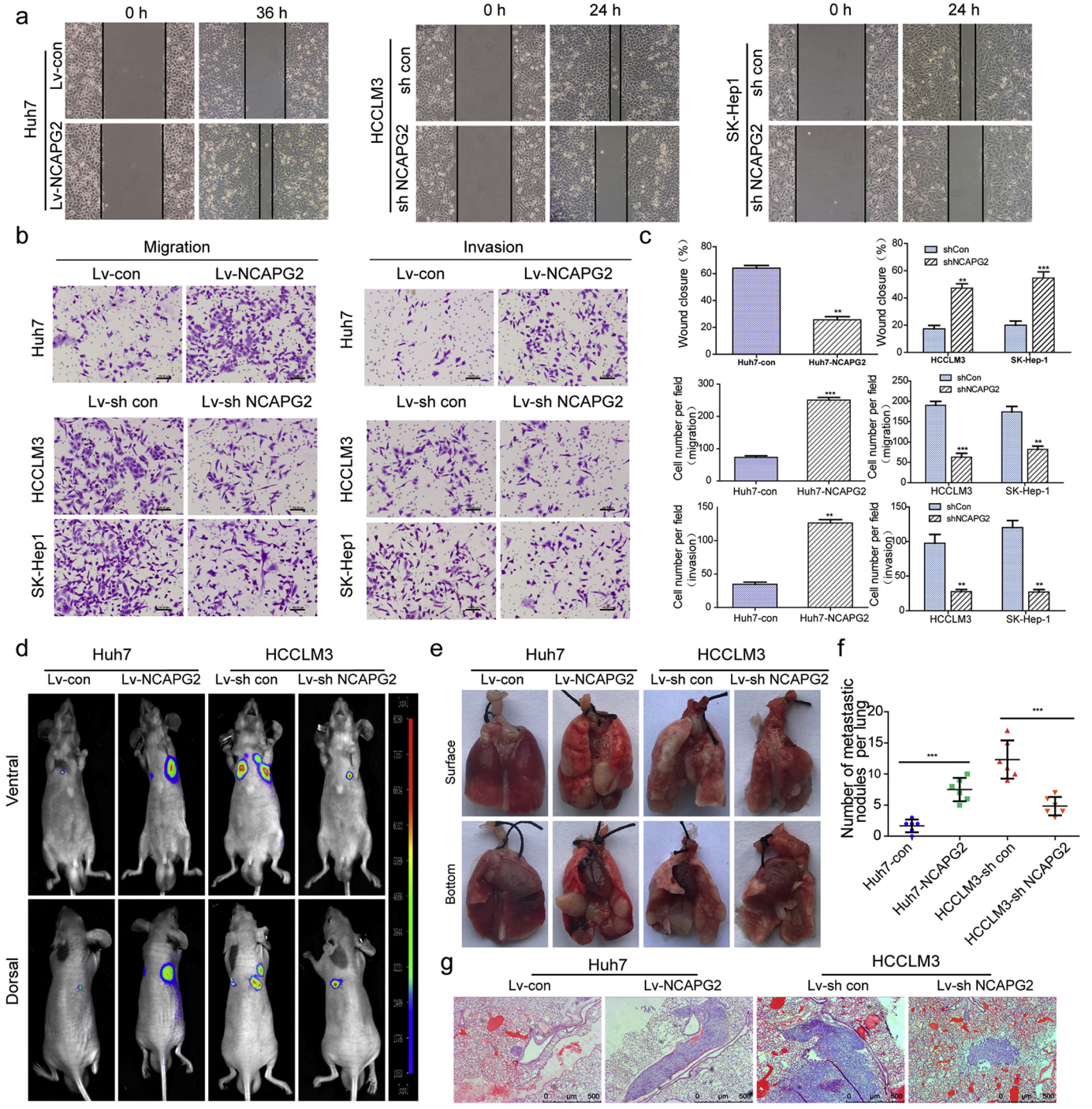

Fig. 3. NCAPG2 promotes HCC cell motility and lung metastasis *in vitro* and *in vivo*. (a) Wound healing assays show that motility is enhanced in Huh7-NCAPG2 cells, whereas NCAPG2 knockdown suppresses motility in HCCLM3 and SK-Hep1 cells. (b) Representative images of Transwell migration and Matrigel invasion assay for the indicated cells (100×). (c) Statistical analysis of the wound healing and Transwell assays for three independent experiments. (d) Representative bioluminescence imaging of lung metastasis derived from tail injection with indicated cells. (e) Representative images of lung metastasis specimens; NCAPG2 overexpression formed more and larger metastatic nodules, whereas NCAPG2 knockdown displayed fewer and smaller nodules. (f) Statistical analysis of lung metastatic foci numbers in different groups ($n = 6$/group) (g) H&E stained images of lung metastasis in the indicated groups. All experiments were performed three times and data are presented as mean ± SD. $^{**}p < .01$; $^{***}p < .001$.

was increased after IL-6 stimulation in a dose- and time-dependent manner in Huh7 cells (Fig. 5g and Supplementary Fig. 7d), indicating that NCAPG2 could promote its own expression by activating STAT3, thus forming a positive feedback loop. To validate the relationship between NCAPG2 and p-STAT3, we detected their expression levels in 80 paired HCC specimens by IHC (Fig. 5h). The Spearman's correlation test confirmed a positive association between NCAPG2 and p-STAT3 in HCC (Fig. 5i). ($r = 0.6101$, $P < .001$).

3.8. NCAPG2 is negatively regulated by miR-188-3p in HCC

More than one-third of all human genes are regulated by miRNAs that play important roles in the progression and metastasis of multiple cancers [29,30]. We screened for miRNAs that could potentially regulate NCAPG2 by analysing several online miRNA target analysis algorithms (Supplementary Fig. 8a). An examination of these miRNAs in HCC liver tumour and adjacent tissues revealed that miR-188-3p is

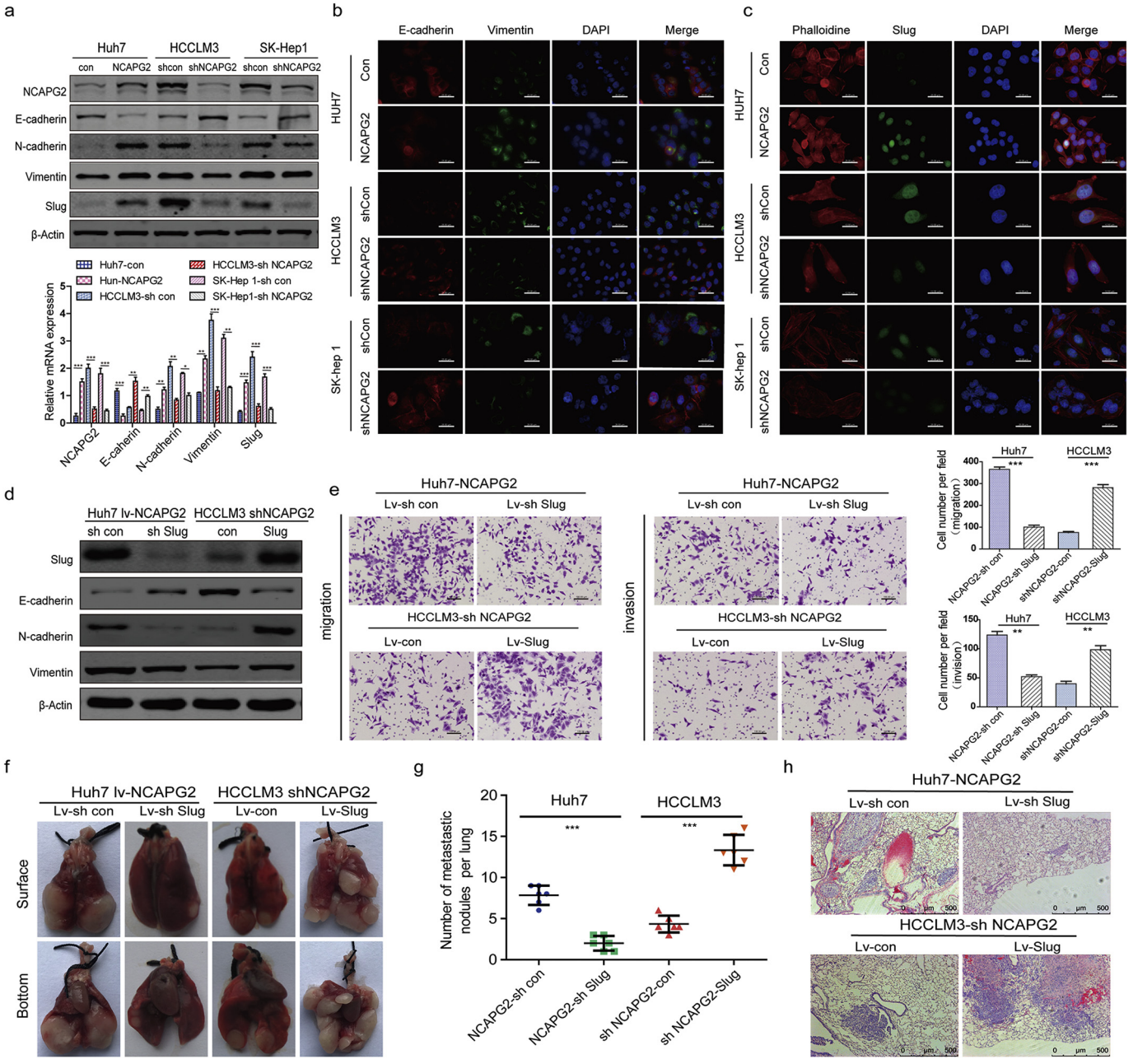

Fig. 4. NCAPG2 induces EMT in a Slug-dependent manner. (a) Western blotting and real-time PCR showed the expression of EMT-associated proteins and mRNAs. (b) Representative IF images of E-cadherin and vimentin expression in the indicated HCC cell lines. (c) Representative IF images of Slug and morphological changes by phalloidine. (d) Western blotting analysis of EMT markers after Slug upregulation or silencing in Huh7-NCAPG2 and HCCLM3-shNCAPG2 cells. Slug knockdown reverses the downregulation of E-cadherin and upregulation of N-cadherin and vimentin induced by NCAPG2 overexpression in Huh7 cells. Slug overexpression reverses the effects caused by NCAPG2 silencing in HCCLM3 cells. (e) Representative images of Transwell migration and invasion after Slug upregulation or silencing in Huh7-NCAPG2 and HCCLM3-shNCAPG2 cells (100×). Statistical analysis of cell numbers is listed in the right panel. (f, g) Representative images of lung metastasis *in vivo* and statistical analysis of metastatic foci numbers in the indicated mouse groups. (h) Images showing representative H&E staining of lung tissue samples from the different experimental groups (n = 6/group). All experiments were performed three times and data are presented as mean ± SD. $^{**}p < .01$; $^{***}p < .001$.

the only miRNA frequently downregulated in HCC (Fig. 6a and Supplementary Fig. 8b-e). We found that the level of miR-188-3p decreases progressively from normal liver cells to HCC cells with low metastatic potential, and finally to HCC cells with high metastatic potential (Supplementary Fig. 9a). Hence, we speculated that the upregulation of NCAPG2 in HCC may be partially attributed to the low level of miR-188-3p. To test this hypothesis, we knocked down and overexpressed miR-188-3p with inhibitors in Huh7 cells and mimics in HCCLM3 and SK-Hep1 cells, respectively. We observed a negative relationship between NCAPG2 and miR-188-3p levels, accompanied by p-STAT3 upregulation and downregulation, respectively (Fig. 6b). To confirm a direct interaction between miR-188-3p and the 3'UTR of *NCAPG2* mRNA, we designed wild-type and mutated sequences of the 3'UTR for luciferase-reporter assays (Fig. 6c). In the wild-type 3' UTR group, miR-188-3p overexpression suppresses Luciferase activity significantly, while the miR-188-3p inhibitor enhances it. In contrast, there is no visible difference in the mutant group (Fig. 6d, e). These data indicate that in HCC, NCAPG2 is negatively regulated by miR-188-3p and decreased miR-188-3p could upregulate NCAPG2 expression.

3.9. MiR-188-3p reverses NCAPG2-mediated proliferation and metastasis in vitro and in vivo

To confirm that miR-188-3p is involved in the tumour-promoting function of NCAPG2, rescue experiments were designed. Colony formation and Transwell Matrigel invasion assays showed that overexpression of miR-188-3p significantly reverses the ability of NCAPG2 to promote proliferation and invasiveness of Huh7-NCAPG2 cells. In contrast, downregulation of miR-188-3p enhances the aggressiveness of HCCLM3-shNCAPG2 cells (Fig. 6f-h and Supplementary Fig. 9b and 10b). Meanwhile, western blotting showed that overexpression of miR-188-3p partly abolishes the Huh7-NCAPG2-induced loss of E-cadherin and upregulation of N-cadherin, vimentin, and Slug (Fig. 6i), which also rescues the morphological changes in Huh7-NCAPG2 and HCCLM3-shNCAPG2 cells (Supplementary Fig. 10a). These results were also confirmed by IF (Fig. 6j). In a liver subcutaneous and orthotopic tumour xenograft model using stable lentiviral transfected cells, we found that an increased level of miR-188-3p attenuates HCC tumorigenesis and growth of Huh7-NCAPG2 cells (Fig. 6g and Supplementary Fig. 9c-e). Mice in the Huh7-NCAPG2-miR-188-3p group have fewer and smaller metastatic lung nodules, compared to the Huh7-NCAPG2-con group (Fig. 6k and Supplementary Fig. 10c, d). H&E staining of the lung sections confirmed these observations (Supplementary Fig. 10f). The enhanced expression of NF-κB, p-NF-κB, p-STAT3, c-myc, cyclin D1, CDK4, and Slug by NCAPG2 overexpression is partly reversed by stable transfection of miR-188-3p in the tumour tissues (Supplementary Fig. 9f and 10e). Moreover, tumour growth and lung metastasis capacities are enhanced in HCCLM3-shNCAPG2 cells by downregulating miR-188-3p expression. Taken together, these results indicate that miR-188-3p can reverse NCAPG2-mediated proliferation and metastasis in HCC.

3.10. NCAPG2 downregulates miR-188-3p and forms a negative feedback loop

It has been reported that miR-188-3p can be suppressed by the activation of NF-κB in a mouse model [31]. Considering that NCAPG2 overexpression activates NF-κB, we asked whether NCAPG2 could regulate miR-188-3p expression by regulating NF-κB activation. Intriguingly, a real-time PCR analysis showed that miR-188-3p expression in Huh7-NCAPG2 cells was suppressed, and that this suppressive effect was restored by si-NF-κB transfection compared to controls (Fig. 7a). Additionally, the upregulation of miR-188-3p expression induced by knocking down NCAPG2 expression in HCCLM3 and SK-Hep1 cells was eliminated by preincubating the cells with TNFα (10 ng/ml, 24 h), which is an NF-κB activator (Fig. 7b). Western blotting confirmed that NCAPG2 expression is enhanced by TNFα-stimulated NF-κB activation in Huh7 cells and the opposite effect is achieved by si-NF-κB in HCCLM3 cells (Fig. 7c). Furthermore, we performed IHC to detect the expression levels of NCAPG2 and p-NF-κB in 80 HCC tissue specimens (Fig. 7d). The Spearman's correlation test revealed a positive relationship between NCAPG2 and p-NF-κB in HCC tissue specimens. ($r =$

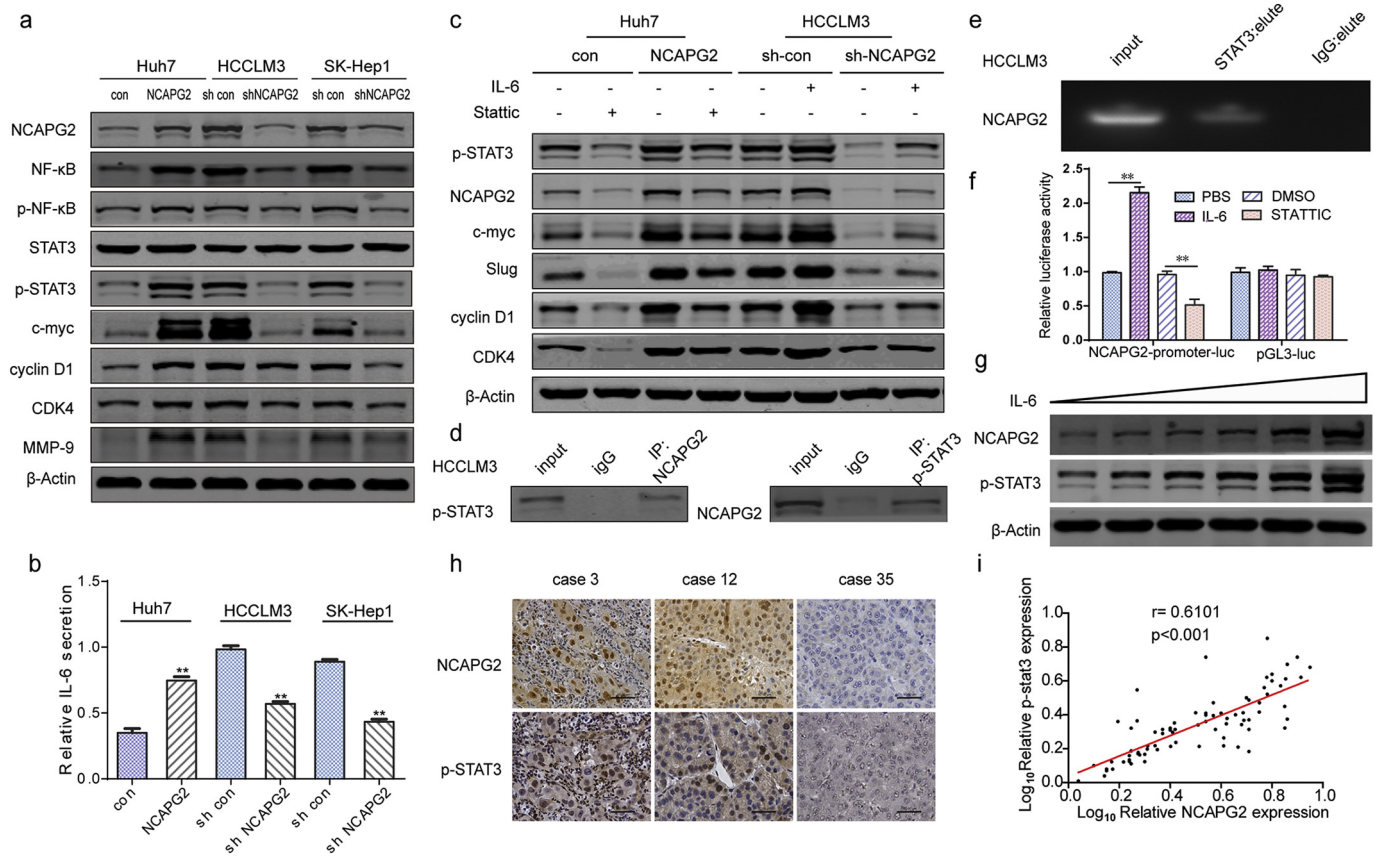

Fig. 5. NCAPG2 activates both the STAT3 and NF-κB signalling pathways. (a) Western blotting of key molecules in several signalling pathways. Overexpression of NCAPG2 enhances the expression of NF-κB, p-NF-κB, p-STAT3, and its target genes (including c-myc, slug, cyclin D1, and CDK4). (b) ELISA results show NCAPG2 overexpression stimulates the secretion of IL-6 in Huh7 cells, whereas knockdown of NCAPG2 suppresses the secretion of IL-6 in HCCLM3 and SK-Hep1 cells. (c) Huh-NCAPG2 cells preincubated with a STAT3 inhibitor (Stattic, 10 μM, 24 h) show downregulation of c-myc, CDK4, cyclin D1, and Slug. When stimulated by IL-6 (10 ng/ml, 24 h), higher expression of p-STAT3 is detected and rescues shRNA-NCAPG2-mediated loss of c-myc, cyclin D1, CDK4, and Slug in HCCLM3 cells. (d) Co-IP assay indicates that NCAPG2 interacts with p-STAT3 in HCCLM3 cells. (e) Chip-qPCR assay shows STAT3 can bind to the NCAPG2 promoter regulatory region. (f) Luciferase reporter assay was performed in HCCLM3 cells transfected of NCAPG2-promoter-luc or pGLC3-luc after IL-6 or Stattic stimulation. (g) NCAPG2 expression is enhanced by IL-6 in a dose-dependent (0, 5, 10, 20, 50, 100 ng/ml, 24 h) manner in Huh7 cells. (h) Representative images from IHC staining analysis of NCAPG2 and p-STAT3 expression in 80 HCC tissues (200×). (i) Correlation analysis between NCAPG2 expression and p-STAT3 levels in 80 patients with HCC by IHC.All experiments were performed three times and data are presented as mean ± SD. $^{**}P < .01$.

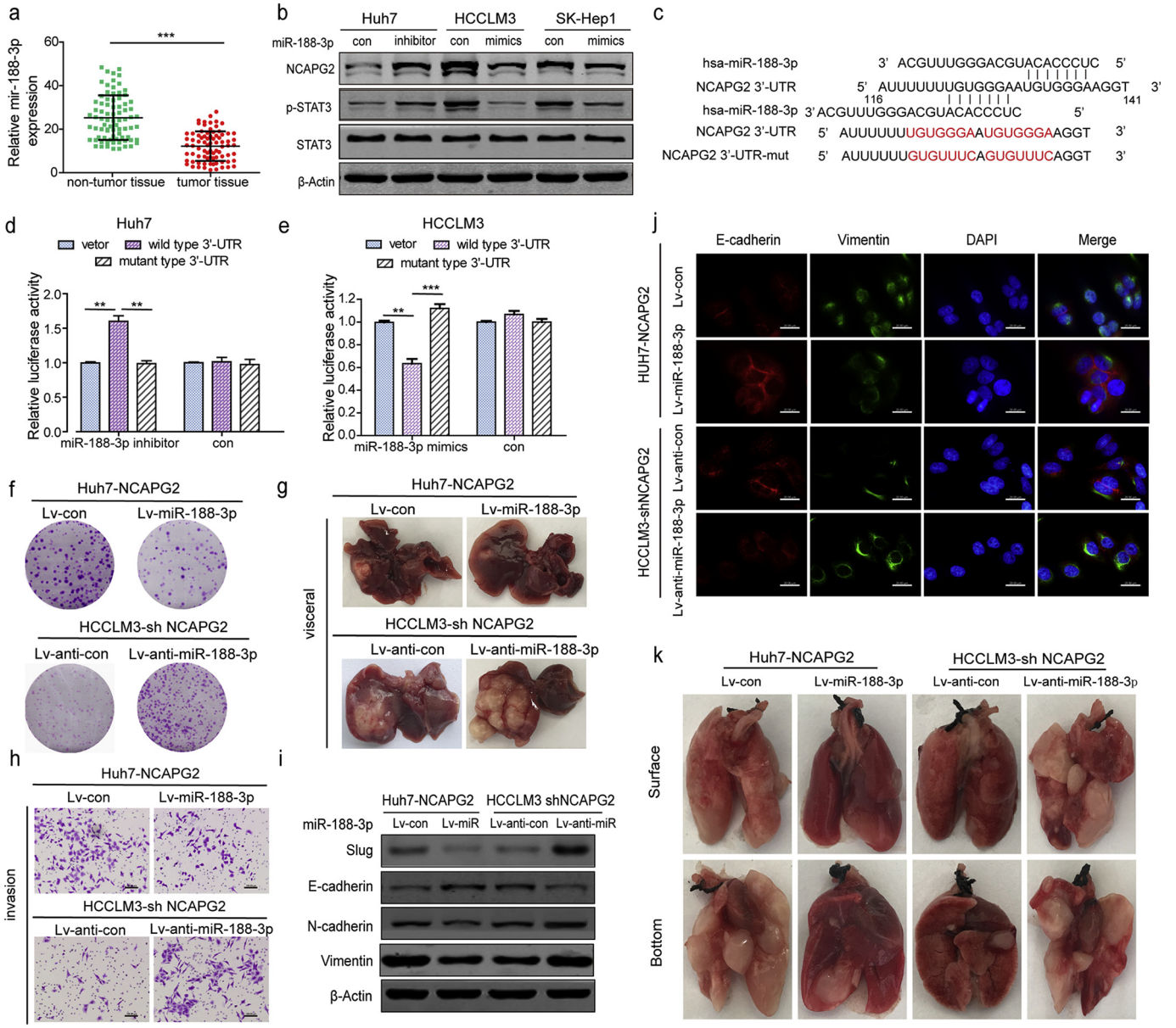

Fig. 6. NCAPG2 is negatively regulated by miR-188-3p. (a) Real-time PCR analysis of miR-188-3p expression in 80 paired HCC and adjacent normal liver tissues. (b) Western blotting show miR-188-3p overexpression suppresses NCAPG2 expression, whereas inhibiting miR-188-3p upregulates NCAPG2 expression. (c) The putative binding sites between miR-188-3p and wild-type or mutant NCAPG2 3'-UTR sequences. (d, e) Luciferase activity assay was performed to confirm the direct binding of miR-188-3p and NCAPG2. (f) Representative images of colony formation after miR-188-3p overexpression or knockdown in Huh7-NCAPG2 and HCCLM3-shNCAPG2 cells. (g) Representative images of liver tumour orthotopic xenografts in the indicated groups (n = 6/group). (h) Representative images of Transwell Matrigel invasion assay in different HCC cells (100×). (i) Western blotting show that miR-188-3p overexpression reverses the upregulation of Slug, N-cadherin and vimentin, and downregulation of E-cadherin induced by NCAPG2 overexpression in Huh7 cells, while knocking down miR-188-3p expression has the opposite effect in HCCLM3-shNCAPG2 cells. (j) Representative IF images of E-cadherin and vimentin in the indicated HCC cells (200×). (k) Representative photographs of lung metastatic tumours from the indicated groups (n = 6/group). All experiments were performed three times and data are presented as mean ± SD. $^{**}P < .01$; $^{***}P < .001$.

0.4806, $P < .001$) (Fig. 7e). These findings indicate the existence of a negative feedback loop between miR-188-3p and NCAPG2 that is dependent on NF-κB activation.

3.11. Combination of miR-188-3p and NCAPG2 has a better prognostic value for HCC

Given the reciprocal relationship between miR-188-3p and NCAPG2 described above, we analysed their expression levels in clinical HCC samples and found a negative correlation between miR-188-3p and NCAPG2 ($r = -0.4389$, $p < .001$) (Fig. 7f). Moreover, patients with low miR-188-3p and high NCAPG2 levels exhibit worse outcomes. In contrast, patients with high miR-188-3p and low NCAPG2 levels had better OS and DFS (Figs. 7g, h). Using a combination of these two parameters increases the prognostic value, compared to using NCAPG2 alone.

4. Discussion

HCC is one of the most common life-threatening neoplasias with high incidence and mortality worldwide; therefore, identifying the molecular targets and mechanisms of HCC is critical to advancing treatment for patients. In this study, we demonstrated that NCAPG2 is a potent oncogene responsible for HCC proliferation and metastasis and is driven predominantly by activation of the STAT3 and NF-κB pathways. Activated STAT3 directly stimulates *NCAPG2* transcription *via* binding to its promoter regulatory region. NCAPG2 overexpression may also be

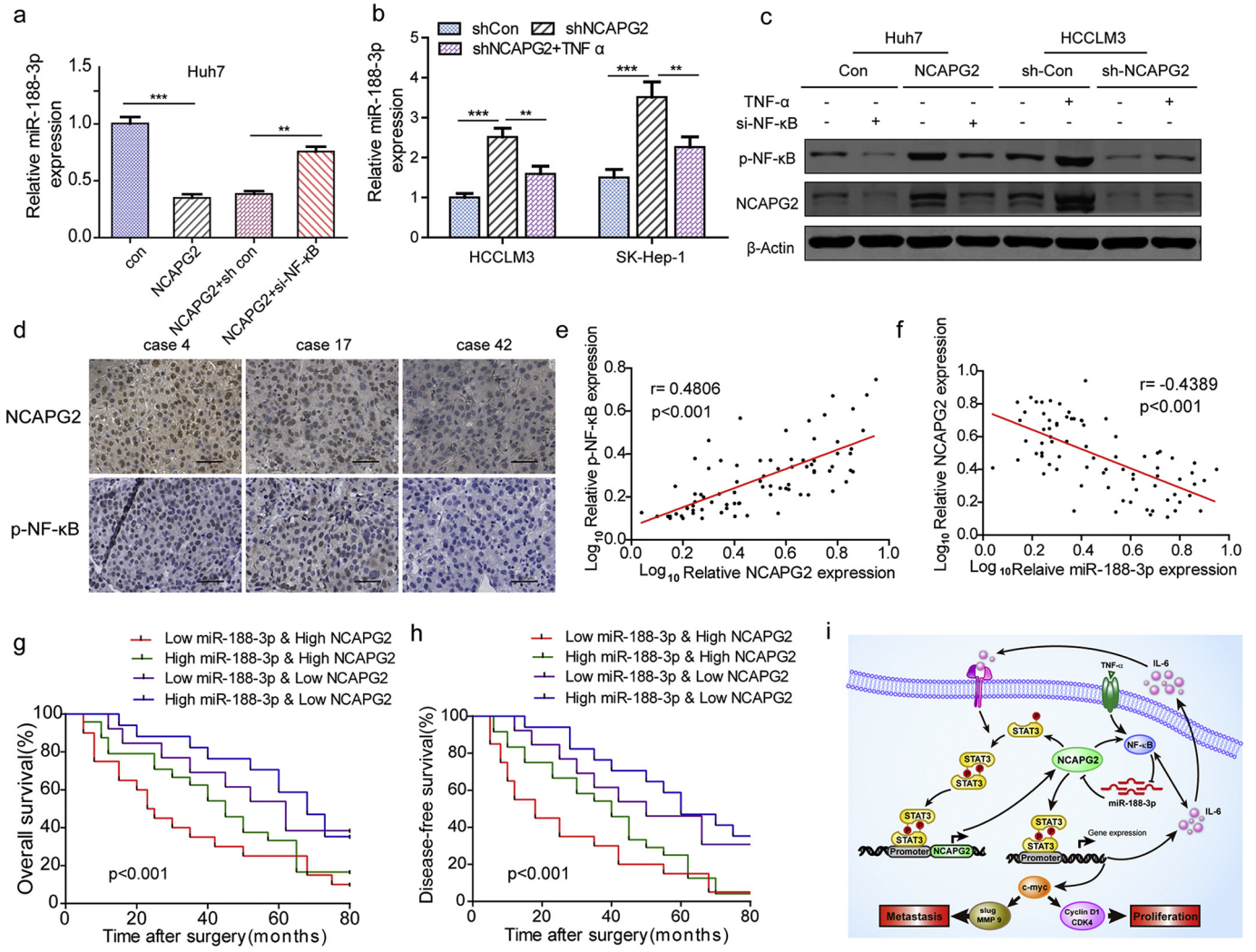

Fig. 7. NCAPG2 downregulates miR-188-3p by activating NF-κB and combination of miR-188-3p and NCAPG2 has a better prognostic value. (a) NCAPG2 overexpression inhibits the expression level of miR-188-3p, whereas NF-κB knockdown rescues the downregulation of miR-188-3p. (b) Real-time PCR show that knocking down NCAPG2 results in upregulated miR-188-3p expression, while the effects are reversed by TNFα (10 ng/ml, 24 h). (c) Western blotting reveals that knocking down NF-κB expression downregulates NCAPG2 expression in Huh-NCAPG2 cells and stimulation by TNFα (10 ng/ml, 24 h) restores the downregulation of NCAPG2 in HCCLM3-shNCAPG2 cells. (d) Representative images of IHC staining analysis of NCAPG2 and p-NF-κB expression in 80 HCC tissues (200×). (e, f) The correlation between NCAPG2 expression and p-NF-κB, NCAPG2, and miR-188-3p levels was analysed in 80 patients. (g, h) Kaplan–Meier analysis of OS and DFS in patients with variable expressions of NCAPG2 and miR-188-3p. (i) Schematic presentation of the mechanism underlying NCAPG2-facilitated HCC proliferation and metastasis. $^{**}p < .01$; $^{***}p < .001$.

partially attributed to reduced miR-188-3p resulting from NF-κB activation. Our findings suggest that NCAPG2 and miR-188-3p play vital roles in HCC progression (Fig. 7i).

NCAPG2 is a component of the condensin II complex that contributes to mitosis and many cellular functions including regulation of gene expression [4,5,32]. It has been reported that NCAPG2 promotes lung adenocarcinoma proliferation and is associated with poor prognosis [7]. Here, we selected NCAPG2 as a promising research target through mRNA microarray and TCGA data analysis from HCC patients. Accordingly, our data show that high expression of NCAPG2 is linked to worse OS and DFS in patients with HCC.

We confirmed that knocking down NCAPG2 expression arrests HCC cells in G1/S-phase and reduces their migration and invasion ability, both *in vitro* and *in vivo*, and suppresses HCC cell tumorigenesis, proliferation, and metastasis in a mouse model. To determine if the reduced migration and invasion was attributed to cell cycle arrest, we designed CCK8 growth curve tests and found that the meaningful growth difference was detected at least 72 h after stable lentivirus transfection of HCC cells, while the migration and invasion tests were conducted no >36 h after transfection, specifically in serum-free medium that restricts HCC cell growth. Furthermore, in liver orthotopic xenograft tumour models, the overexpressing NCAPG2 groups exhibited a higher number of intrahepatic metastatic nodules than the controls. Conversely, knocking down NCAPG2 resulted in fewer intrahepatic metastatic nodules. Therefore, our results indicate that NCAPG2 plays a significant role in both HCC proliferation and metastasis.

On the molecular level, our investigation uncovered the role of NCAPG2 in regulating EMT *via* enhancing the expression of the mesenchymal markers N-cadherin and vimentin, and decreasing the expression of the epithelial maker E-cadherin during HCC migration and invasion. This involvement of NCAPG2 in EMT is dependent on the transcription factor Slug. Moreover, both the STAT3 and NF-κB pathways are involved in NCAPG2-mediated HCC proliferation and metastasis, rather than the ERK and AKT pathways. NCAPG2 increases the phosphorylation of STAT3, resulting in upregulation of c-myc, CDK4, cyclin D1, Slug, and MMP9, which are important tumour growth and metastasis promoting factors, consistent with recent studies [33,34]. C-myc is an important transcription factor that directly upregulates CDK4, cyclin D1, Slug, and MMP9 expression [35–37]. Moreover, phosphorylation of STAT3 can activate NANOG expression and NANOG can induce Slug expression at the transcriptional level [38]. However, further

investigation is required to elucidate the relationship between p-Stat3 and Slug in HCC.

We also found that activated STAT3 could directly bind to the NCAPG2 promotor regulatory region and upregulate NCAPG2 expression to establish a positive feedback loop. In addition, activated NF-κB is always associated with HCC proliferation, EMT, MMP activity, angiogenesis, and metastasis. Interestingly, STAT3 and NF-κB can be mutual regulators that depend on IL-6 to a certain extent. Previous studies have reported that both STAT3 and NF-κB can bind directly to the IL-6 promoter to upregulate IL-6 expression, and IL-6 also stimulates STAT3 and NF-κB activation [19,33,39,40]. In this study we found that IL-6 is upregulated and downregulated after overexpressing and silencing NCAPG2 expression, respectively. Thus, we hypothesise that NCAPG2 participates in the crosstalk between the STAT3 and NF-κB pathways, and plan to investigate this in the future.

Accumulating evidence indicate that miRNAs play indispensable roles in tumour development and progression by inducing either translational repression or mRNA degradation [29]. MiR-188-3p was found to have multiple functions in diverse diseases, including regulating autophagy suppression [41] and neurodegenerative disease [31], and acting as an oncogene in colorectal cancer [42]. Here, we found that miR-188-3p is frequently downregulated in HCC tissues compared to adjacent normal liver tissues, and we confirmed that miR-188-3p directly targets NCAPG2 to negatively regulate NCAPG2 expression and blocks NCAPG2-mediated HCC proliferation and metastasis. It was previously reported that miR-188-3p expression could be suppressed by NF-κB activation [31], and consistent with that, our results showed that miR-188-3p is negatively regulated by NCAPG2 in a manner dependent on the enhanced activation of NF-κB, thereby forming a negative feedback loop. Finally, the combination of high NCAPG2 and low miR-188-3p expression is correlated with a worse prognosis in patients with HCC.

In conclusion, we demonstrated for the first time that NCAPG2 is an important oncogene that contributes to HCC proliferation and metastasis. NCAPG2 can activate both the STAT3 and NF-κB pathways and activated STAT3 positively regulates NCAPG2 expression. Moreover, overexpression of NCAPG2 is a consequence of reduced miR-188-3p, which is closely associated with activated NF-κB. There exists a positive regulation loop between NCAPG2 and p-STAT3 and a negative regulation loop between NCAPG2 and miR-188-3p. These results provide a foundation for understanding the mechanism of HCC progression and may contribute to the identification of new biomarkers and therapeutic targets for HCC.

Supplementary data to this article can be found online at https://doi.org/10.1016/j.ebiom.2019.05.053.

Acknowledgments and Funds

National Key Program for Science and Technology Research and Development (Grant No. 2016YFC0905902); the National Natural Scientific Foundation of China (Nos. 81772588, 81602058, 81773194); University Nursing Program for Young Scholars with Creative Talents in Heilongjiang Province (Grant No. UNPYSCT-2016200); innovative Research Program for Graduate of Harbin Medical University (Grant Nos. YJSCX2017-38HYD, YJSCX2016-18HYD).

Conflict of interests

The authors declare no conflict of interest.

Authors' contributions

Concept and design: MFZ, ZSG, SRP, LY.
Performed the experiments: MFZ, HJH, LXY, LYF, ZF, MK, ZCY.
Data analysis and interpretation: YGC, PSH, WJZ, WY, CYF, ZB.
Writing and review of Manuscript: MFZ, SRP, LYJ, SX, LZY.
Article revise:MFZ. ZSG. SYF, XMY.
Supervision: WJB, LLX.
Final approval of manuscript: All authors.

References

[1] Siegel RL, Miller KD, Jemal A. Cancer statistics, 2017. CA Cancer J Clin 2017;67(1):7–30.
[2] Chen Q, Shu C, Laurence AD, et al. Effect of Huaier granule on recurrence after curative resection of HCC: a multicentre, randomised clinical trial. Gut 2018;67(11):2006–16.
[3] Serper M, Taddei TH, Mehta R, et al. Association of Provider Specialty and Multidisciplinary Care with Hepatocellular Carcinoma Treatment and mortality. Gastroenterology 2017;152(8):1954–64.
[4] Liu W, Tanasa B, Tyurina OV, et al. PHF8 mediates histone H4 lysine 20 demethylation events involved in cell cycle progression. Nature 2010;466(7305):508–12.
[5] Kim JH, Shim J, Ji MJ, et al. The condensin component NCAPG2 regulates microtubule-kinetochore attachment through recruitment of polo-like kinase 1 to kinetochores. Nat Commun 2014;5:4588.
[6] Studach LL, Rakotomalala L, Wang WH, et al. Polo-like kinase 1 inhibition suppresses hepatitis B virus X protein-induced transformation in an in vitro model of liver cancer progression. Hepatology 2009;50(2):414–23.
[7] Zhan P, Xi GM, Zhang B, et al. NCAPG2 promotes tumour proliferation by regulating G2/M phase and associates with poor prognosis in lung adenocarcinoma. J Cell Mol Med 2017;21(4):665–76.
[8] Bartel DP. MicroRNAs: target recognition and regulatory functions. Cell 2009;136(2):215–33.
[9] Gonzalez-Vallinas M, Breuhahn K. MicroRNAs are key regulators of hepatocellular carcinoma (HCC) cell dissemination-what we learned from microRNA-494. Hepatobiliary surgery and nutrition 2016;5(4):372–6.
[10] Huang J, Wang Y, Guo Y, Sun S. Down-regulated microRNA-152 induces aberrant DNA methylation in hepatitis B virus-related hepatocellular carcinoma by targeting DNA methyltransferase 1. Hepatology 2010;52(1):60–70.
[11] Chai S, Ng KY, Tong M, et al. Octamer 4/microRNA-1246 signaling axis drives Wnt/beta-catenin activation in liver cancer stem cells. Hepatology 2016;64(6):2062–76.
[12] Zhou JN, Zeng Q, Wang HY, et al. MicroRNA-125b attenuates epithelial-mesenchymal transitions and targets stem-like liver cancer cells through small mothers against decapentaplegic 2 and 4. Hepatology 2015;62(3):801–15.
[13] Alpini G, Glaser SS, Zhang JP, et al. Regulation of placenta growth factor by microRNA-125b in hepatocellular cancer. J Hepatol 2011;55(6):1339–45.
[14] Trinchieri G. Cancer and inflammation: an old intuition with rapidly evolving new concepts. Annu Rev Immunol 2012;30:677–706.
[15] Huynh J, Chand A, Gough D, Ernst M. Therapeutically exploiting STAT3 activity in cancer - using tissue repair as a road map. Nat Rev Cancer 2019;19:82–96.
[16] Song R, Song H, Liang Y, et al. Reciprocal activation between ATPase inhibitory factor 1 and NF-kappaB drives hepatocellular carcinoma angiogenesis and metastasis. Hepatology 2014;60(5):1659–73.
[17] Uthaya Kumar DB, Chen CL, Liu JC, et al. TLR4 Signaling via NANOG cooperates with STAT3 to activate Twist1 and promote formation of tumor-initiating stem-like cells in livers of mice. Gastroenterology 2016;150(3):707–19.
[18] Lee H, Herrmann A, Deng JH, et al. Persistently activated Stat3 maintains constitutive NF-kappaB activity in tumors. Cancer Cell 2009;15(4):283–93.
[19] Yoon S, Woo SU, Kang JH, et al. NF-kappaB and STAT3 cooperatively induce IL6 in starved cancer cells. Oncogene 2012;31(29):3467–81.
[20] Iliopoulos D, Hirsch HA, Struhl K. An epigenetic switch involving NF-kappaB, Lin28, Let-7 MicroRNA, and IL6 links inflammation to cell transformation. Cell 2009;139(4):693–706.
[21] Han J, Wang F, Lan Y, et al. KIFC1 regulated by miR-532-3p promotes epithelial-to-mesenchymal transition and metastasis of hepatocellular carcinoma via gankyrin/AKT signaling. Oncogene 2019;38(3):406–20.
[22] Puisieux A, Brabletz T, Caramel J. Oncogenic roles of EMT-inducing transcription factors. Nat Cell Biol 2014;16(6):488–94.
[23] Stemmler MP, Eccles RL, Brabletz S, Brabletz T. Non-redundant functions of EMT transcription factors. Nat Cell Biol 2019;21(1):102–12.
[24] Zhang H, Song Y, Yang H, et al. Tumor cell-intrinsic Tim-3 promotes liver cancer via NF-kappaB/IL-6/STAT3 axis. Oncogene 2018;37(18):2456–68.
[25] Ning BF, Ding J, Liu J, et al. Hepatocyte nuclear factor 4alpha-nuclear factor-kappaB feedback circuit modulates liver cancer progression. Hepatology 2014;60(5):1607–19.
[26] Wang X, Sun W, Shen W, et al. Long non-coding RNA DILC regulates liver cancer stem cells via IL-6/STAT3 axis. J Hepatol 2016;64(6):1283–94.
[27] Liu S, Sun X, Wang M, et al. A microRNA 221- and 222-mediated feedback loop maintains constitutive activation of NFkappaB and STAT3 in colorectal cancer cells. Gastroenterology 2014;147(4):847–59 e11.
[28] McDaniel JM, Varley KE, Gertz J, et al. Genomic regulation of invasion by STAT3 in triple negative breast cancer. Oncotarget 2017;8(5):8226–38.
[29] Hammond SM. An overview of microRNAs. Adv Drug Deliv Rev 2015;87:3–14.
[30] Berindan-Neagoe I, Calin GA. Molecular pathways: microRNAs, cancer cells, and microenvironment. Clinical cancer research 2014;20(24):6247–53.
[31] Zhang J, Hu M, Teng Z, Tang YP, Chen C. Synaptic and cognitive improvements by inhibition of 2-AG metabolism are through upregulation of microRNA-188-3p in a mouse model of Alzheimer's disease. J Neurosci 2014;34(45):14919–33.
[32] Khan TN, Khan K, Sadeghpour A, et al. Mutations in NCAPG2 cause a severe neurodevelopmental syndrome that expands the phenotypic Spectrum of Condensinopathies. Am J Hum Genet 2019;104(1):94–111.

[33] Yan Q, Jiang L, Liu M, et al. ANGPTL1 interacts with integrin alpha1beta1 to suppress HCC angiogenesis and metastasis by inhibiting JAK2/STAT3 Signaling. Cancer Res 2017;77(21):5831–45.
[34] Steder M, Alla V, Meier C, et al. DNp73 exerts function in metastasis initiation by disconnecting the inhibitory role of EPLIN on IGF1R-AKT/STAT3 signaling. Cancer Cell 2013;24(4):512–27.
[35] Zhang Z, Zhu P, Zhou Y, et al. A novel slug-containing negative-feedback loop regulates SCF/c-kit-mediated hematopoietic stem cell self-renewal. Leukemia 2017;31(2):403–13.
[36] Anders L, Ke N, Hydbring P, et al. A systematic screen for CDK4/6 substrates links FOXM1 phosphorylation to senescence suppression in cancer cells. Cancer Cell 2011;20(5):620–34.
[37] Pello OM, De Pizzol M, Mirolo M, et al. Role of c-MYC in alternative activation of human macrophages and tumor-associated macrophage biology. Blood 2012;119(2):411–21.
[38] Yao C, Su L, Shan J, et al. IGF/STAT3/NANOG/slug Signaling Axis simultaneously controls epithelial-Mesenchymal transition and Stemness maintenance in colorectal Cancer. Stem Cells 2016;34(4):820–31.
[39] Marotta LL, Almendro V, Marusyk A, et al. The JAK2/STAT3 signaling pathway is required for growth of CD44(+)CD24(−) stem cell-like breast cancer cells in human tumors. J Clin Invest 2011;121(7):2723–35.
[40] Chang R, Song L, Xu Y, et al. Loss of Wwox drives metastasis in triple-negative breast cancer by JAK2/STAT3 axis. Nat Commun 2018;9(1):3486.
[41] Wang K, Liu CY, Zhou LY, et al. APF lncRNA regulates autophagy and myocardial infarction by targeting miR-188-3p. Nat Commun 2015;6:6779.
[42] Pichler M, Stiegelbauer V, Vychytilova-Faltejskova P, et al. Genome-wide miRNA analysis identifies miR-188-3p as a novel prognostic marker and molecular factor involved in colorectal carcinogenesis. *Clinical cancer research: an official journal of the American Association for*. Cancer Res 2017;23(5):1323–33.